
Inter-Quark Potential

BY BEN COUSER (908293)

College of Science, Swansea University

ABSTRACT

Using the Nambu-Goto string action associated for curved space-time and radial component of $AdS_5 \times S^5$ we can find expectation values similar to the rectangular Wilson loop operator. In the t' Hooft limit we find a dual theory between gauge theory and IIB string theory. In the limit that $T \rightarrow \infty$, a rectangular Wilson loop's expectation value is related to the potential energy between a quark-antiquark pair. We study the background of the AdS/CFT correspondence field and how different metrics yield different relations between the energy and separation of quarks in meson pairs. We propose a metric that describes the true relationship found through experiment.

Contents

1	Introduction	1
2	Wilson Loops in Large N Field Theories	2
2.1	Wilson Loops and the Relation to Supergravity	2
2.2	Prescription for Quark Anti-Quark Potential	4
3	Confinement	6
4	Full Inter-Quark Potential	7
4.1	Asymptotic Behaviour	7
4.2	Inter-Quark Potential	9
5	Numerical Analysis	11
6	Conclusions	13
7	References	14
8	Appendix	15

1 Introduction

Quantum field theory states that the fundamental building blocks of the universe are fluctuation of fields that correspond to particles. Each particle having its own individual field. String theory extends the point particle into a 1 dimensional string that can be open like a guitar string, or closed like an elastic band. Different modes of vibrations correspond to different particles. The first hint of a string theory came in the 1960's when experiments were finding large amounts of mesons and hadrons that followed Regge slopes. These slopes showed that the mass square of the particles were directly proportion to their angular momentum [1]. Veneziano used this relation to postulate a scattering amplitude formula that corresponded with string interactions. This was known as the first string revolution and was before the discovery of quarks. Once quarks were found, quantum chromodynamics (QCD) became the leading theory of how the strong force interacted with quarks. Though at high energies the theory broke down. QCD is described by a group of 3×3 , special, unitary matrices named $SU(3)$. Where each quark has three generations of colours charge and anti-colour partners. Gerard t' Hooft postulated that one could solve the theory where the number of colour gluons $N \rightarrow \infty$, while keeping $g_{YM}^2 N$ constant, known as the t' Hooft coupling constant. Note that the reason that we have a factor of N in the coupling is because there are N gluon types now that can transfer force between quarks [2]. If $N = 3$ could be compared to $N = \infty$ then this would give reason to why Regge trajectory is analogous to modes of string vibration. Implying that the large N limit connects gauge theories to a type of string theory (IIB), known as holography. The holographic principal in string theory is the notion that quantum gravity in a space-time volume can be dual to a lower dimensional quantum field theory on the surface of the surface of space-time.

AdS_5 is the maximally symmetric solution to Einstein's equation but superstrings can only propagate in 10 dimensions. Therefore we must add 5 more dimensions to our universe [3]. Since the gauge theory $SU(4) \approx SO(6)$ global symmetry, it is natural to have the extra 5 dimensions on a 5-Sphere. Thus a $\mathcal{N} = 4$ super Yang-Mills theory could be the same as a superstring theory of $AdS_5 \times S^5$. Note that for our large N limit to dual to string theory we must have our radius of our 5-sphere to be sufficiently large in string units [6]. The goal of this paper is to calculate the expectation value of the Wilson loop operator for a metric that will give the provide a relationship for the inter-quark potential against the separation between them. [4,5].

2 Wilson Loops in Large N Field Theories

2.1 Wilson Loops and the Relation to Supergravity

To begin finding an expression for the potential it was essential to review Juan Maldacena's paper that pioneered the approach that will be prescribed, "Wilson Loops in Large N Field Theories" [4]. The Wilson Loop Operator for a Yang-Mills theory is the trace path-ordered exponential gauge field A along a contour,

$$W(C) = \frac{1}{N} \text{Tr} P e^{i \oint_C A}. \quad (2.1)$$

Where C is a closed rectangular loop through spacetime that is on the surface of our 5-sphere, as represented in figure 1.

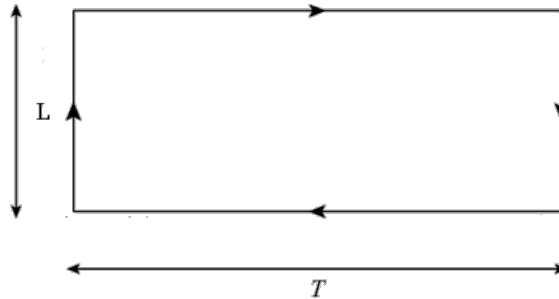


Figure 1: The Wilson loop contour

The Wilson loop is considered as a phase factor associated with the propagation of very massive quarks that are situated on the boundary of the 5-sphere. In the limit $T \rightarrow \infty$ the expectation value for the Wilson loop operator is

$$\langle W(C) \rangle \sim e^{-TE(L)}, \quad (2.2)$$

where $E(L)$ is the potential energy stored between a quark anti-quark pair separated by a distance L . In order to calculate equation 2.2, it is required to added massive quarks. To do so we will break the symmetry $U(N+1) \rightarrow U(N) \times U(1)$ by assigning some expectation value to the Higgs field, $\vec{\Phi}$. It is intuitive to think that the masses of our quarks is proportional to this expectation value and in the limit where $|\vec{\Phi}| \rightarrow \infty$ it is clear that the masses will tend to infinity. As required to be able to compute Wilson loops in $U(N)$ theory [4].

By relating this to supergravity it is logical to assume

$$\langle W(C) \rangle \sim e^{-S}, \quad (2.3)$$

where S is the action of a the string which is proportional to the proper area of the world sheet in the constant t' Hooft coupling. By comparing the two expressions (2) and (3) we find the relation

$$S = TE(L). \quad (2.4)$$

However, if we work out the proper distance of the string we end up with an integral that diverges to infinity. This should not come as a surprise as we first assumed that the quarks were situated at the boundary of our 5-sphere which is where $U = \infty$. Instead what we must do is take some arbitrary cut off U_m which is analogous to the mass terms of the quarks. This is depicted in figure 2. By subtracting these mass terms from our Wilson loop operator we find,

$$\langle W(C) \rangle \sim \lim_{U_m \rightarrow \infty} e^{S_{U_m} - LU_m}, \quad (2.5)$$

where L is the total length of the Wilson loop and U_m is the mass of the quark and our proper length becomes finite.

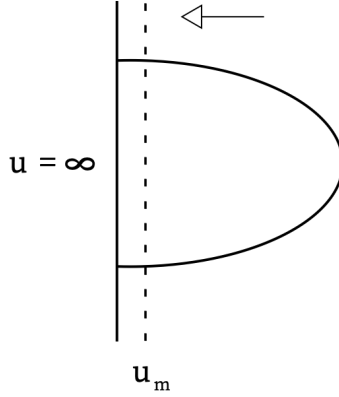


Figure 2: Configuration to show cut off where $U \rightarrow \infty$

2.2 Prescription for Quark Anti-Quark Potential

We will now calculate the Wilson Loop of figure 1 in the limit that $T \rightarrow \infty$ so the problem becomes translational invariant in the T direction. The Nambu-Goto [4] representation for the string world sheet is

$$S = \frac{1}{2\pi\alpha'} \int d\tau d\sigma \sqrt{\det G_{MN} \partial_\alpha X^M \partial_\beta X^N}, \quad (2.6)$$

with G_{MN} being the metric tensor for the Euclidean $AdS_5 \times S^5$ metric

$$ds^2 = \alpha' \left[\frac{U^2}{R^2} (dt^2 + dx_i dx_i) + \frac{R^2}{U^2} dU^2 + R^2 d\Omega_5^2 \right]. \quad (2.7)$$

The radius of our 5-sphere, $R = (4\pi g_s N)^{\frac{1}{4}}$, is in string units and $U = r/\alpha'$ has dimensions of energy. Where the string coupling $g_s = g_{YM}^2/2\pi$. By taking a static gauge we can relate $\tau = t, \sigma = x$. The action becomes

$$S = \frac{T}{2\pi} \int dx \sqrt{(\partial_x U)^2 + U^4/R^4}. \quad (2.8)$$

Using the fact that the Lagrangian is not explicitly dependant on x , we may use the relation

$$constant = \frac{\partial \mathcal{L}}{\partial(\partial_x U)} (\partial_x U) - \mathcal{L} \quad (2.9)$$

leading us to the condition,

$$constant = \frac{U^4}{\sqrt{(\partial_x U)^2 + U^4/R^4}}. \quad (2.10)$$

If we assume that due to symmetry depicted in figure 2, the minimum point of U is situated at $x = 0$, we find the constant

$$\begin{aligned} \partial_x U|_{x(U=U_o)=0} = 0 &\Rightarrow \frac{U_o^4}{\sqrt{(0)^2 + \frac{U_o^4}{R^4}}} = constant = U_o^2 R^2 \\ U_o^2 R^2 &= \frac{U^4}{\sqrt{(\partial_x U)^2 + U^4/R^4}}. \end{aligned} \quad (2.11)$$

Using equation 2.11 we are able to find a solution for the position,

$$x = \frac{R^2}{U_o} \int_1^{U/U_o} \frac{dy}{y^2 \sqrt{y^4 - 1}}, \quad (2.12)$$

where $y = U/U_o$. We are able to find a function for the separation of quarks with

$$\frac{L}{2} = \frac{R^2}{U_o} \int_1^\infty \frac{dy}{y^2 \sqrt{y^4 - 1}} = \frac{R^2}{U_o} \frac{\sqrt{2\pi^{\frac{3}{2}}}}{\Gamma(1/4)^2} \quad (2.13)$$

where $\Gamma(1/4)$ is Euler gamma function,

$$\Gamma(u) = \int_0^\infty t^{u-1} e^{-t} dt. \quad (2.14)$$

If we use this information to find the potential between the quarks we would get a divergent integral. This is because we made the assumption that the quarks were infinite in mass, corresponding to a string that stretches from zero to $U = \infty$. Instead, integrate to a cut off point U_{max} and regularise by subtracting the mass of the two quarks that is $U_{max}/2\pi$,

$$E' = \frac{2}{2\pi} \int_0^{\frac{L}{2}} dx \mathcal{L} = \frac{2}{2\pi} \int_{U_0}^\infty dU \mathcal{L} (\partial_x U)^{-1}. \quad (2.15)$$

We are able to deduce from equation 2.11,

$$\partial_x U = \frac{U^2}{R^2} \sqrt{\frac{U^4}{U_0^4} - 1} \quad (2.16)$$

and so we find our energy before renormalisation to be,

$$E' = \frac{2U_0}{2\pi} \int_1^\infty dy \frac{y^2}{\sqrt{y^4 - 1}}. \quad (2.17)$$

Now we must renormalise the integral and find a true potential between the two quarks.

$$E = \frac{2U_0}{2\pi} \int_1^{y_{max}} dy \frac{y^2}{\sqrt{y^4 - 1}} - \frac{2U_0}{2\pi} \int_0^{y_{max}} dy \quad (2.18)$$

$$E = \frac{2U_0}{2\pi} \int_1^{y_{max}} dy \frac{y^2}{\sqrt{y^4 - 1}} - \frac{2U_0}{2\pi} \left[\int_1^{y_{max}} dy + \int_0^1 dy \right]$$

where $y_{max} = \frac{U_{max}}{U_0}$. Then as $y_{max} \rightarrow \infty$ we find,

$$E = \frac{2U_o}{2\pi} \left[\int_1^\infty dy \left(\frac{y^2}{\sqrt{y^4 - 1}} - 1 \right) - 1 \right] \quad (2.19)$$

$$E = -\frac{4\pi^2(2g_{YM}^2 N)^{\frac{1}{2}}}{\Gamma(1/4)^4 L} \quad (2.20)$$

This agrees with the asymptotic behaviour found at small quark separation and is the first milestone to gain the full relationship of quark potential.

3 Confinement

Colour confinement is the phenomenon where quarks cannot be observed in isolation. When we attempt to separate quarks, non-bound states, so much work is put in that instead of separating them, two new quarks are created from the energy and thus we are left with two quark anti-quark pairs. Thus to have confinement we must have a condition that when the separation between quarks increases, the energy of the system increases linearly with the proportion of linearity being the tension of the string.

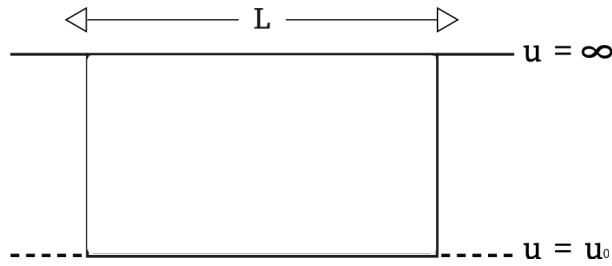


Figure 3: Plot to show real length when $L \rightarrow \infty$

Now let us consider a general case where $U^2 \rightarrow f(U)$. The Nambu-Goto action takes the form [5],

$$S = \frac{T}{2\pi} \int dx \sqrt{(\partial_x U)^2 + f(U)^2} \quad (3.1)$$

where $f(U)$ is an even function with a minimum. For a very large separation $\partial_x U \approx 0$, and $f(U) \approx f(U_0)$. This is depicted in figure 3 and note that the minimum point is at U_0 as it was in §2. Thus for large separation we can approximate that the inter-quark energy is

$$\begin{aligned} E &\approx \frac{1}{2\pi} \int_{-L/2}^{L/2} dx \sqrt{(0)^2 + f(U_0)^2} \\ E &\approx \frac{2}{2\pi} \int_0^{L/2} dx f(U_0) = \frac{f(U_0)}{2\pi} \cdot L \end{aligned} \quad (3.2)$$

where L is their separation. Thus we find in the large separation limit that energy is directly proportional to the energy with constant of proportionality that is analogous to the string tension [5].

4 Full Inter-Quark Potential

4.1 Asymptotic Behaviour

So far we have found two separate cases that agree with both limits of small and large quark anti-quark separation. The goal is to find a metric that yield both asymptotic relationships. It should be noted that separation of quarks is inversely proportional to U_0 as when the quarks are closer together there is a higher minimal value for U . The action is defined as

$$S = \frac{T}{2\pi} \int dx \sqrt{(\partial_x U)^2 + F(U)^2}. \quad (4.1)$$

The essential properties we need for $F(U)$ to properly model inter-quark potential is it must be an even function with a minimum, and at the small L limit we want our expression to simplify to (2.20). To attain both asymptotes the function

$$F(U) = \frac{1}{R^2} \left(U^2 + \frac{\Sigma^2}{U^2} \right) \quad (4.2)$$

was purposed, where Σ is some arbitrary constant. Due to the inverse relationship between separation and U_0 it is clear that

$$\lim_{L \rightarrow 0} S = \frac{T}{2\pi} \int dx \sqrt{(\partial_x U)^2 + \frac{U^4}{R^4}} \quad (4.3)$$

which is identical equation (2.20). Thus has the desired relationship at small separation

$$E \propto -1/L. \quad (4.4)$$

On the other end of the spectrum, at large separation equation (4.1) becomes

$$\lim_{L \rightarrow \infty} S \approx \frac{2T}{2\pi} \int_0^{L/2} dx F(U_0). \quad (4.5)$$

To find the string tension we must determine minimal value of $F(U)$.

$$\begin{aligned} \partial_U F(U) &= \frac{1}{R^2} \left(2U - \frac{2\Sigma^2}{U^3} \right) \\ \partial_U F(U = U_0) &= 0 = \frac{1}{R^2} \left(2U_0 - \frac{2\Sigma^2}{U_0^3} \right) \\ U_0 &= +\sqrt{\Sigma} \end{aligned} \quad (4.6)$$

Notice that the positive root for U_0 was chosen as U is a scalar quantity and therefore cannot be negative. We find that the minimal value of $F(U)$ and the string tension is

$$\begin{aligned} F(U_0) &= \frac{1}{R^2} \left(\Sigma + \frac{\Sigma^2}{\Sigma} \right) \\ F(U_0) &= \frac{2\Sigma}{R^2}. \end{aligned} \quad (4.7)$$

Equation 3.2 can be implemented and lead to

$$E = \frac{\Sigma}{\pi R^2} \cdot L \quad (4.8)$$

This confirms that the purposed function $F(U)$ correctly yields both small and large separation behaviour that is prominent in real world meson potential as found using experiment.

4.2 Inter-Quark Potential

By following the exact same prescription used in §2.2 it is possible to find a relationship for $E(U_0)$ and $L(U_0)$ and numerically solve to find the potential of a meson pair in terms of the quark anti-quark separation. By using the condition, equation 2.9, on the Lagrangian within equation 4.1 it can be shown that

$$constant = \frac{1}{2\pi} \frac{-F(U)^2}{\sqrt{(\partial_x U)^2 + F(U)^2}} = \frac{1}{(2\pi)^2} \frac{F(U)^2}{\mathcal{L}}. \quad (4.9)$$

By using the same rule of symmetry as in §2.2 we can see that

$$\partial_x U|_{x(U=U_0)=0} = 0 \Rightarrow \frac{1}{2\pi} \frac{-F(U_0)^2}{\sqrt{(0)^2 + F(U_0)^2}} = \frac{-F(U_0)}{2\pi} = constant. \quad (4.10)$$

Equating 4.9 and 4.10 we find our geodesic for system,

$$\mathcal{L} = \frac{1}{2\pi} \frac{F(U)^2}{F(U_0)} = \frac{1}{2\pi} \sqrt{(\partial_x U)^2 + F(U)^2}. \quad (4.11)$$

With this we can now solve the differential equation 4.11 to find an expression for the quark separation in terms of the minimal value of U ,

$$\frac{F(U)^2}{F(U_0)} = \sqrt{(\partial_x U)^2 + F(U)^2}$$

$$(\partial_x U)^2 = \frac{F(U)^4}{F(U_0)^2} - F(U)^2$$

leading us to,

$$\partial_x U = \frac{F(U)}{F(U_0)} \sqrt{F(U)^2 - F(U_0)^2}. \quad (4.12)$$

An expression for the proper length is found using,

$$L = \int_{-L/2}^{L/2} dx = 2 \int_{U_0}^{\infty} \frac{dU}{(\partial_x U)}, \quad (4.13)$$

$$L(U_0) = 2 \int_{U_0}^{\infty} dU \frac{F(U_0)}{F(U)} \frac{1}{\sqrt{F(U)^2 - F(U_0)^2}}, \quad (4.14)$$

revealing our final solution for $L(U_0)$. To find an expression of $E(U_0)$ we first must use equation (2.4) to get a naive value for the energy (that will end up being infinite),

$$E' = \int_{-L/2}^{L/2} dx \mathcal{L} = 2 \int_{U_0}^{\infty} dU \frac{\mathcal{L}}{\partial_x U} \quad (4.15)$$

$$E' = \frac{2}{2\pi} \int_{U_0}^{\infty} \frac{F(U)}{\sqrt{F(U)^2 - F(U_0)^2}} dU. \quad (4.16)$$

We are now able to renormalise (4.16) and find the total energy of the configuration in terms of the minimum point U_0 . By integrating up to a cut of U_{max} and subtracting the regularised masses of the quarks we find a finite relationship,

$$E = \frac{2}{2\pi} \int_{U_0}^{U_{max}} \frac{F(U)}{\sqrt{F(U)^2 - F(U_0)^2}} dU - \frac{2}{2\pi} \int_0^{U_{max}} dU$$

Now by taking the limit where $U_{max} \rightarrow \infty$ the relation becomes,

$$E(U_0) = \frac{2}{2\pi} \left[\int_{U_0}^{\infty} dU \left(\frac{F(U)}{\sqrt{F(U)^2 - F(U_0)^2}} - 1 \right) - U_0 \right]. \quad (4.17)$$

Equations 4.14 and 4.17 are both in terms of the parameter U_0 but it is impossible to analytically merge both formulas to give energy in terms of the quark separation. Instead numerical methods must be employed.

5 Numerical Analysis

It happens that $E(L)$ cannot be found analytically. Instead what must be done is input specific values of U_0 into equations (4.14) and (4.17), plotting the results. Before we were able to compute results we define $R = 1$ for simplicities sake. To solve the equations (4.14) and (4.17) Wolfram Mathematica is used to numerically solve these complex integrals. Then we export the data into python console for plotting. To begin we took $\Sigma = 1$ and found the length and energy as pure functions of U_0 in figures 4 and 5.

Now with the framework to find numerical values for $E(U_0)$ and $L(U_0)$ possible it is necessary to find general boundary condition for what U_0 we can have. Clearly if we want real, finite number answers for both separation and energy and thus the denominators in both integrals must be real. Thus we find the condition,

$$F(U) > F(U_0), \quad (5.1)$$

$$U^2 + \frac{\Sigma^2}{U^2} > U_0^2 + \frac{\Sigma^2}{U_0^2}. \quad (5.2)$$

Thus we can conclude that when choosing our limits of integration, we should integrate to a minimal value of $U_0 + \delta U_0$ if analytically solving. Note that in the numerical analysis on the other hand this does not appear to be a problem as when integrating from the minimum U_0 we find finite results. Using the tools acquired we then can export data into a plotting code, figure 10, to visually display the relationship between E, L and U_0 . Table 1 shows the data found when $\Sigma = 1$. Figures 8 and 9 show the discovered relationships for $L(U_0)$ and $E(U_0)$ respectively. By using the plotting code shown in figure 6 we graphically show a relationship between the inter-quark potential and their separation, figure 10.

In order to prove the relationship found does indeed agree with the asymptotic behaviour of a real quark anti-quark pair's potential, we should find two cases. In the large L case it is found that from equation 4.8,

$$\lim_{L \rightarrow \infty} \frac{E}{L} = \frac{\Sigma}{\pi}. \quad (5.3)$$

In the small L case equation 2.20 shows,

$$\lim_{L \rightarrow 0} E \cdot L = -\frac{4\pi^2(2g_{YM}^2 N)^{1/2}}{\Gamma(1/4)^4}. \quad (5.4)$$

To assure figure 10 does in fact follow the limits in equations 5.3 and 5.4 we can plot the left had side quantities against the separation and see if they approach the limits purposed respectively. To plot the found data figure 7 was used in python software. Figure 11 shows that indeed in the large separation case we have the correct relationship. In the small separation limit on the other hand it is not so clear.

In order to prove the small separation case we must first approximate what value $E \cdot L$ is tending to by reading off of figure 12. The constant of proportionality is defined to be

$$\frac{4\pi^2(2g_{YM}^2 N)^{1/2}}{\Gamma(1/4)^4} \approx 0.2285$$

From §2 we know the radius of AdS_5 , $R^2 = (2g_{YM}^2 N)^{1/2}$, and thus can show

$$\begin{aligned} \frac{4\pi^2 R^2}{\Gamma(1/4)^4} &= 0.2285 \\ R &= \frac{\Gamma(1/4)^2}{2\pi} \sqrt{0.2285} = 1.00006 \end{aligned} \quad (5.5)$$

Note that when we began simulations we assumed the radius of AdS curvature, $R = 1$. Therefore we have shown that our purposed function, $F(U)$, yields both ends of asymptotic behaviour.

The next stage of computation was to see how Σ would effect the quark-antiquark potential. The hypothesis is that the relationship will be unchanged at small separation but when in the large separation the gradient would vary depending on equation 5.3. The resultant data found for $\Sigma = 0, 2, 3, 4$ can be found in tables 2, 3, 4 and 5 respectively. Then the graphics for the data found are figures 13 to 31. In order to accurately compare our sigma models to the hypothesis put forward, figure 32 shows all sets of energy and separation data into one graph and fully agrees with the hypothesis. We see is that all sigma models look the same for small separation, as would be assumed and all models would tend to the large distance limit (5.3) including the case put forward in [4].

6 Conclusions

To begin this project we looked at the field of AdS/CFT correspondence, or more accurately how quantum gravity in a spacetime volume could be dual to a quantum field theory on the surface of such volume [4,6]. In the 't Hooft limit, [2], we discovered that a $SU(N)$ symmetry, where $N = 3$, can be compared to the type IIB string theory, when $N \rightarrow \infty$ while $g_{YM}^2 N$ remains constant. Through studying [4] we see that in this limit we find the expectation value of the Wilson loop operator in the limit that $T \rightarrow \infty$ corresponds to the Nambu-Goto string action of the worldsheet whose boundary lies on the loop in study. Using Euler-Lagrangian mechanics we show that in $AdS_5 \times S^5$ that the quark potential is inversely proportional to the separation which we noted to be the true relationship in the small separation limit. Reviewing [5] show that we can make the transformation, $U^2 \rightarrow f(U)$, in our metric where our purposed function, $f(U)$, is real, non negative and has a minimum. In the large separation limit we have confinement where $f(U_0)$ corresponds to the string tension in the large N limit. Using both [4,5] we proposed a transformation $U^2 \rightarrow F(U)$ in § 4. This transformation yielded the small and large limit behaviours as required and we were able to find the energy and separation in terms of the minimal point of U_0 .

It was not possible to analytically find a formula for energy in terms of quark separation. Therefore we numerically found the relationship for $\Sigma = 0, 1, 2, 3, 4$. This was a suboptimal solution as it meant it would take a lot longer to repeatedly input data and we would have to numerically evaluate the integrals. We programmed our expressions for energy and separation in terms of the U_0 with Mathematica software as it is extremely advanced and intuitive to use. Once sufficient data was found we graphically displayed the resultant relationships in figures 13 to 31. We discovered that our model followed a relationship that strongly resembled real world data found in experiment, shown in figures 10, 15, 20 and 25. In the small separation limit, we hypothesised that all sigma models tend to the Maldacena case [4]. Comparing figures 12, 17, 22 and 27 to figure 31 proved that for all $\Sigma > 1$ models, as the separation decreased, the relationship would tend to the Maldacena relationship. With this information we were able accurately find the earlier assumption that $R = 1$ in equation 5.5. Indicating that this model of universe could in fact be possible. The final conclusion we can make from the results found is that the value of sigma only has influence on the gradient of the relationship in the

large separation limit. Figure 32 clearly reflects this. The property that we are able to effect one end of the relationship while keeping the other constant is extremely useful and opens the possibility to future fine tune sigma, fitting our model to the true natural relationship found via experiment. Being able to analytically solve for $E(L)$ would be a great triumph for future as two key limitations of the computation was the limited data points. This would allow fitting to real data to be much easier.

7 References

Acknowledgments

First and foremost I am very grateful to my supervisor Adi Armoni for providing me great insight and understanding into this field. I would like to thank Swansea University for providing me the opportunity to take part in this project. I would finally like to thank Jemima Couser for creating graphics to help illustrate my ideas.

- [1] M. B. Green, J. H. Schwarz, E. Witten, "Superstring Theory," . Cambridge University Press (1987)
- [2] G. 't Hooft, "A Planar Diagram Theory for Strong Interactions," *Nucl. Phys.* **B72** (1974) 461.
- [3] O. Aharony, S. S. Gubser, J. Maldacena, H. Ooguri, Y. Oz, "Large N Field Theories, String Theory and Gravity" *Phys. Rept.* **323**,183 (2000)
- [4] J. Maldacena, "Wilson Loops in Large N Field Theories", *Phys. Rev. Lett.* 80 (1998) 4859-4862, hep-th/9803002
- [5] Y. Kinar, E. Schreiber and J. Sonnenschein, "QQ Potential from Strings in Curved Spacetime - Classical Results"" hep-th/9811192
- [6] J. Maldacena, "The Large N Limit of Superconformal field theories and supergravity", *International journal of theoretical physics* 38.4 (1999): 1113-1133

8 Appendix

List of Tables

1	$\Sigma = 1$	17
2	$\Sigma = 2$	18
3	$\Sigma = 3$	19
4	$\Sigma = 4$	20
5	$\Sigma = 0$	21

List of Figures

1	The Wilson loop contour	2
2	Configuration to show cut off where $U \rightarrow \infty$	3
3	Plot to show real length when $L \rightarrow \infty$	6
4	$L(U_0, \Sigma = 1)$	22
5	$L(U_0, \Sigma = 1)$	22
6	Plotting code a	23
7	Plotting code b	23
8	$L(U_0, \Sigma = 1)$	24
9	$E(U_0, \Sigma = 1)$	24
10	$E(L, \Sigma = 1)$	25
11	$E(U_0, \Sigma = 1)/L(U_0, \Sigma = 1), BlackLine = 1/\pi$	25
12	$E(U_0, \Sigma = 1) \cdot L(U_0, \Sigma = 1)$	26
13	$L(U_0, \Sigma = 2)$	27
14	$E(U_0, \Sigma = 2)$	27
15	$E(L, \Sigma = 2)$	28
16	$E(U_0, \Sigma = 2)/L(U_0, \Sigma = 2), BlackLine = 2/\pi$	28
17	$E(U_0, \Sigma = 2) \cdot L(U_0, \Sigma = 2)$	29
18	$L(U_0, \Sigma = 3)$	30
19	$E(U_0, \Sigma = 3)$	30
20	$E(L, \Sigma = 3)$	31
21	$E(U_0, \Sigma = 3)/L(U_0, \Sigma = 3), BlackLine = 3/\pi$	31
22	$E(U_0, \Sigma = 3) \cdot L(U_0, \Sigma = 3)$	32
23	$L(U_0, \Sigma = 4)$	33
24	$E(U_0, \Sigma = 4)$	33
25	$E(L, \Sigma = 4)$	34

26	$E(U_0, \Sigma = 4)/L(U_0, \Sigma = 4), BlackLine = 4/\pi$	34
27	$E(U_0, \Sigma = 4) \cdot L(U_0, \Sigma = 4)$	35
28	$L(U_0, \Sigma = 0)$	36
29	$E(U_0, \Sigma = 0)$	36
30	$E(L, \Sigma = 0)$	37
31	$E(U_0, \Sigma = 0) \cdot L(U_0, \Sigma = 0)$	37
32	$E(L, \Sigma = 0, 1, 2, 3, 4)$	38

Table 1: $\Sigma = 1$

U_0	L	E
1.000000001	9.63636	2.59386
1.000000005	9.5879	2.57844
1.000000001	9.58908	2.54735
1.000000005	8.72971	2.30527
1.000000009	8.46964	2.22248
1.0000001	9.41924	2.52475
1.0000005	7.64766	1.96084
1.0000009	7.35185	1.86668
1.000009	6.20398	1.5013
1.000089	5.05867	1.13674
1.00089	3.90761	0.770346
1.0089	2.75836	0.404516
1.089	1.62864	0.0437732
1.2	1.25386	-0.0796193
1.3	1.07688	-0.141553
1.4	0.957152	-0.186668
1.5	0.868055	-0.223176
2	0.614458	-0.356769
2.5	0.484217	-0.464362
3	0.401363	-0.564963
3.5	0.343241	-0.662952
4	0.300004	-0.759774
4.5	0.266513	-0.85601
5	0.239782	-0.951923
5.5	0.217939	-1.04765
6	0.199752	-1.14326
6.5	0.184371	-1.23879
7	0.171191	-1.33427
7.5	0.159772	-1.42972
8	0.149782	-1.52515
8.5	0.140968	-1.62055
9	0.133135	-1.71595
9.5	0.126126	-1.81133
10	0.119819	-1.90671

Table 2: $\Sigma = 2$

U_0	L	E
1.414214	5.56939	2.87597
1.41422	4.62777	2.27652
1.4143	3.70986	1.69216
1.415	2.92931	1.19525
1.45	1.58405	0.338688
1.5	1.28168	0.145553
1.6	1.02214	-0.0223026
1.8	0.790238	-0.179501
2	0.666791	-0.271911
2.5	0.499801	-0.425242
3	0.407438	-0.5431
3.5	0.346017	-0.649384
4	0.30142	-0.750748
4.5	0.267297	-0.849693
5	0.240243	-0.947328
5.5	0.218225	-1.0442
6	0.199937	-1.1406
6.5	0.184495	-1.2367
7	0.171277	-1.3326

Table 3: $\Sigma = 3$

U_0	L	E
1.732051	4.83257	3.79467
1.73206	3.73433	2.74593
1.7321	3.25032	2.28373
1.733	2.39599	1.46791
1.74	1.78309	0.882619
1.8	1.16895	0.295755
2	0.791047	-0.0703746
2.5	0.528633	-0.352116
3	0.418034	-0.504718
3.5	0.350754	-0.626141
4	0.303811	-0.735462
4.5	0.268613	-0.839062
5	0.241017	-0.93962
5.5	0.218704	-1.03843
6	0.200246	-1.13617
6.5	0.184702	-1.23322
7	0.17142	-1.32982

Table 4: $\Sigma = 4$

U_0	L	E
2.00001	3.24897	3.18975
2.0001	2.67347	2.457
2.001	2.09791	1.72417
2.01	1.52283	0.991955
2.1	0.95315	0.265862
2.2	0.786691	0.0517963
2.4	0.626929	-0.159239
2.6	0.538439	-0.283106
2.8	0.478576	-0.373336
3	0.434028	-0.446353
3.5	0.357636	-0.592196
4	0.307229	-0.713539
4.5	0.270479	-0.823954
5	0.242109	-0.928724
5.5	0.219379	-1.03029
6	0.200681	-1.12993
6.5	0.184993	-1.22832
7	0.17162	-1.3259

Table 5: $\Sigma = 0$

U_0	L	E
0.1	11.9814	-0.019069
0.25	4.79256	-0.0476725
0.5	2.39628	-0.095345
0.75	1.59752	-0.143017
1	1.19814	-0.19069
2	0.59907	-0.38138
3	0.39938	-0.57207
4	0.299535	-0.76276
5	0.239628	-0.95345
6	0.19969	-1.14414
7	0.171163	-1.33483
8	0.149768	-1.52552
9	0.133127	-1.71621
10	0.119814	-1.9069

```

Out[14]= 1

Out[15]= 1

In[14]:= f[u_] := (u^2 + (1/(u^2)))

In[15]:= Function[u, u^2 + 1/u^2]

Out[15]= Function[u, u^2 + 1/u^2]

In[43]:= l[uo_] := 2 * NIntegrate[(f[uo]/f[u]) * (1/Sqrt[f[u]^2 - f[uo]^2]), {u, uo, Infinity}]

In[44]:= Function[uo, 2 NIntegrate[f[uo]/(f[u] Sqrt[f[u]^2 - f[uo]^2]), {u, uo, infinity}]]

Out[44]= Function[uo, 2 NIntegrate[f[uo]/(f[u] Sqrt[f[u]^2 - f[uo]^2]), {u, uo, infinity}]]

In[45]:= Function[uo, 2 NIntegrate[f[uo]/(f[u] Sqrt[f[u]^2 - f[uo]^2]), {u, uo, infinity}]] [2]

Out[45]= 0.614458

```

Figure 4: $L(U_0), \Sigma = 1$

```

In[46]:= e[uo_] :=
  (1/(Pi)) * ((NIntegrate[(f[u]/Sqrt[f[u]^2 - f[uo]^2]) - 1, {u, uo, Infinity}]) - uo)

In[47]:= Function[uo, (NIntegrate[f[u]/(Sqrt[f[u]^2 - f[uo]^2]) - 1, {u, uo, infinity}] - uo)/Pi]

Out[47]= Function[uo, (NIntegrate[f[u]/(Sqrt[f[u]^2 - f[uo]^2]) - 1, {u, uo, infinity}] - uo)/Pi]

In[48]:= Function[uo, (NIntegrate[f[u]/(Sqrt[f[u]^2 - f[uo]^2]) - 1, {u, uo, infinity}] - uo)/Pi] [2]

Out[48]= -0.356769

```

Figure 5: $L(U_0), \Sigma = 1$


```

## sigma = 1

import matplotlib.pyplot as plt

uo = [1.000000005,1.00000005,1.0000005,1.000000001,1.00000001,1.00000001,1.00000009,1.0000009,1.000009,1.000089,1.00089,1.0089,1.0089,1.089,1.2,1.3,1.4,1.5,2,2.5,3,3.5,4,4.5,5,5.5,6,6.5,7,7.5,8,8.5,9,9.5,10]

l = [9.5879,8.72971,7.64766,9.63636,9.58908,9.41924,8.46964,7.35185,6.20398,5.05867,3.90761,2.75836,1.62864,1.25386,1.07688,0.957152,0.868055,0.614458,0.484217,0.401363,0.343241,0.300004,0.266513,0.239782,0.217939,0.199752,0.184371,0.171191,0.159772,0.149782,0.140968,0.133135,0.126126,0.119819]

E = [2.57844,2.30527,1.96084,2.59386,2.54735,2.52475,2.22248,1.86668,1.5013,1.13674,0.770346,0.404516,0.0437732,-0.0796193,-0.141553,-0.186668,-0.223176,-0.356769,-0.464362,-0.564963,-0.662952,-0.759774,-0.85601,-0.951923,-1.04765,-1.14326,-1.23879,-1.33427,-1.42972,-1.52515,-1.62055,-1.71595,-1.81133,-1.90671]

plt.scatter(uo,l,marker=".")
plt.xlabel('Uo')
plt.ylabel('Separation')
plt.show()

plt.scatter(uo,E,marker=".")
plt.xlabel('Uo')
plt.ylabel('Energy')
plt.show()

plt.scatter(l,E,marker=".")
plt.xlabel('Separation')
plt.ylabel('Energy')
plt.show()

```

Figure 6: Plotting code a

```

m = []

for i in range(34):
    e = E[i]
    L = l[i]
    d = e/L
    m.append(d)

plt.scatter(l,m,marker=".")
plt.plot([0,10],[0.31831,0.31831], 'k-',lw=0.5)
plt.xlabel('Separation')
plt.ylabel('Energy/Separation')
plt.show()

n = []

for i in range(34):
    e = E[i]
    L = l[i]
    c = e * L
    n.append(c)

print(n)

plt.scatter(l,n,marker=".")
plt.xlabel('Separation')
plt.ylabel('Energy * Separation')
plt.show()

```

Figure 7: Plotting code b

$$\underline{\Sigma = 1}$$

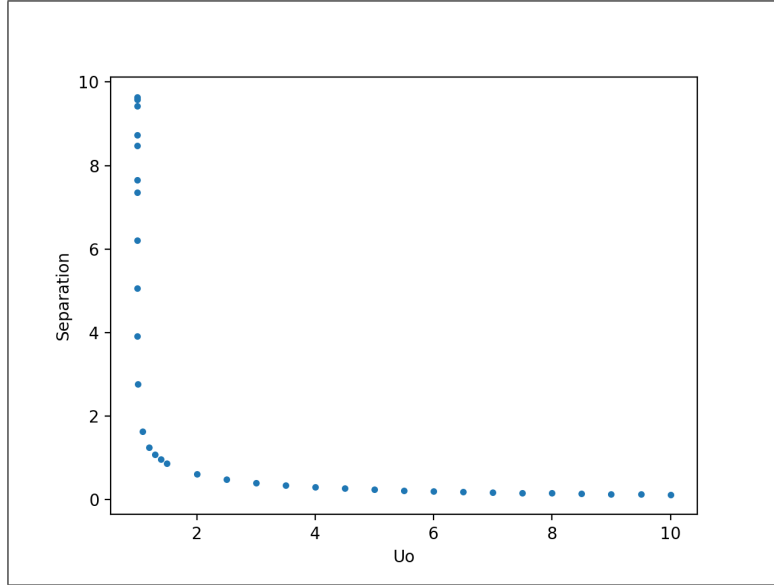


Figure 8: $L(U_0, \Sigma = 1)$

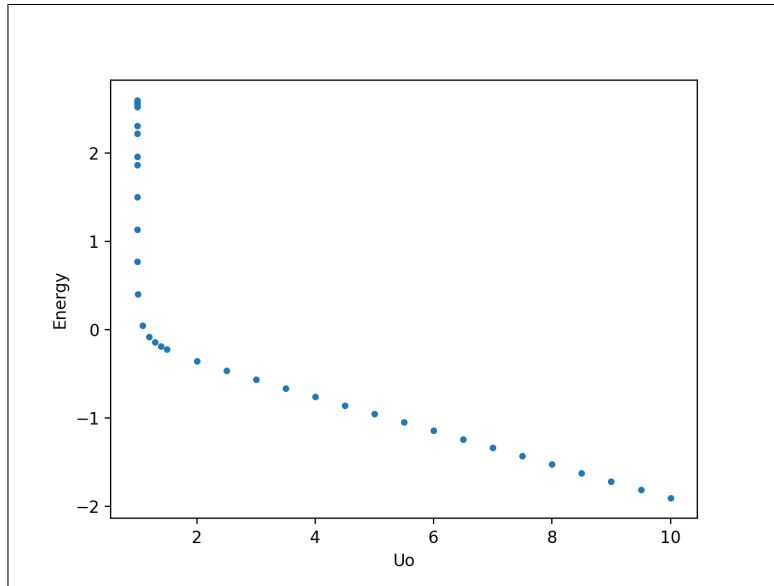


Figure 9: $E(U_0, \Sigma = 1)$

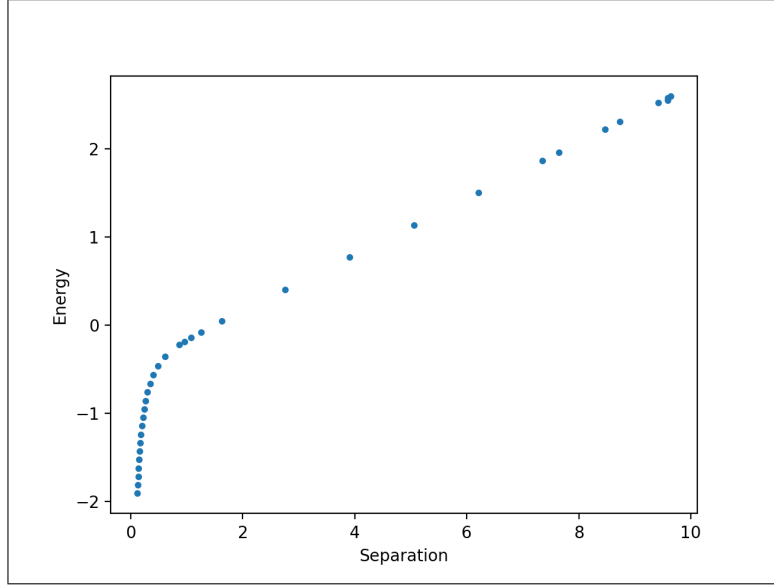


Figure 10: $E(L, \Sigma = 1)$

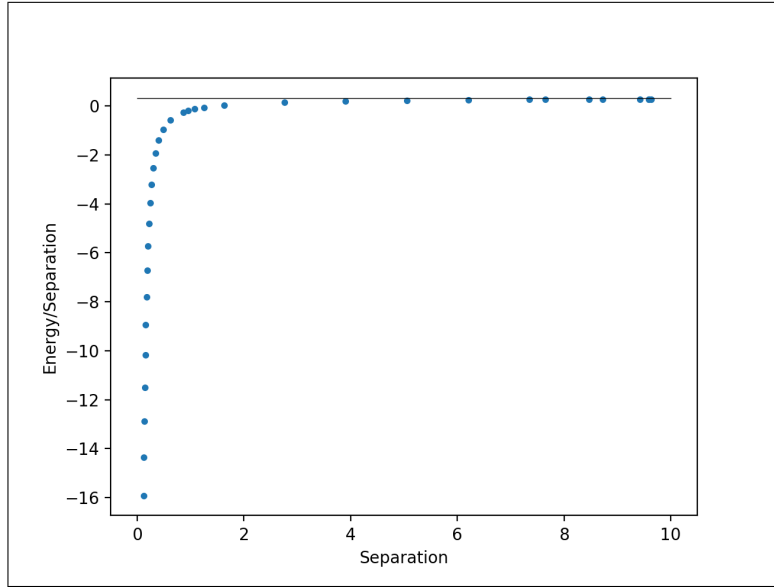


Figure 11: $E(U_0, \Sigma = 1)/L(U_0, \Sigma = 1)$, *BlackLine* = $1/\pi$

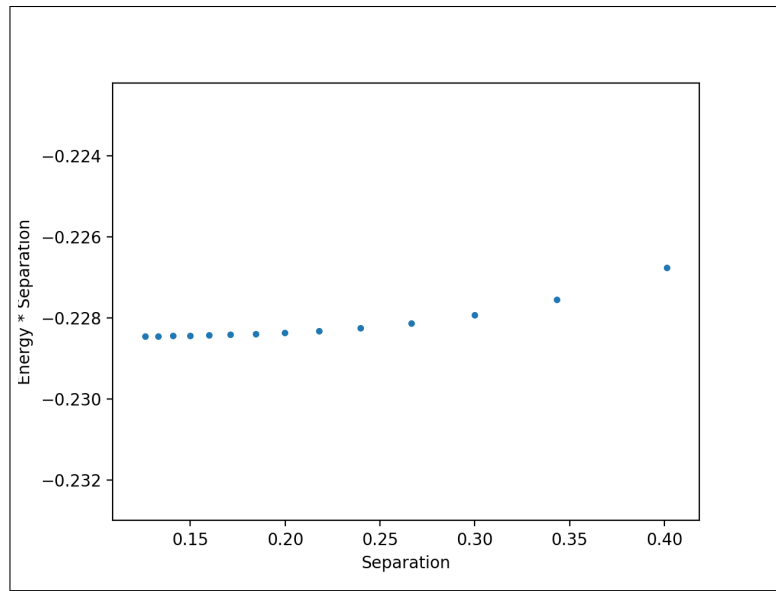


Figure 12: $E(U_0, \Sigma = 1) \cdot L(U_0, \Sigma = 1)$

$$\underline{\Sigma = 2}$$

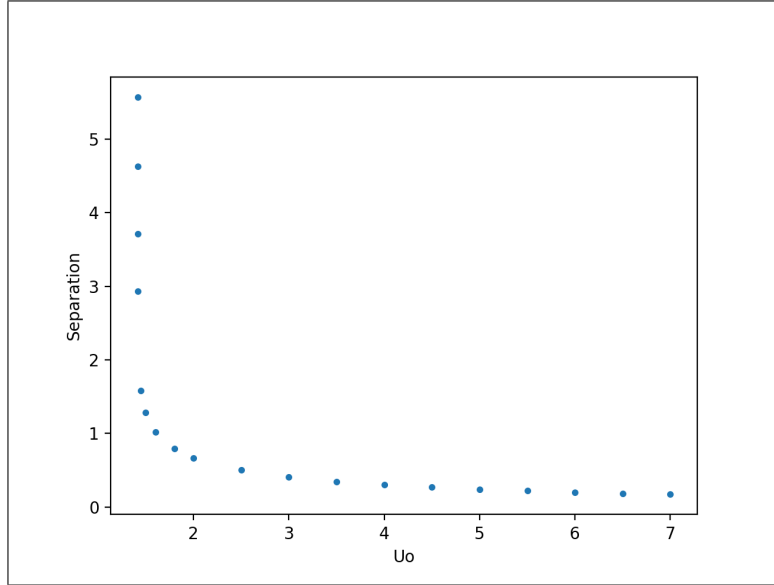


Figure 13: $L(U_0, \Sigma = 2)$

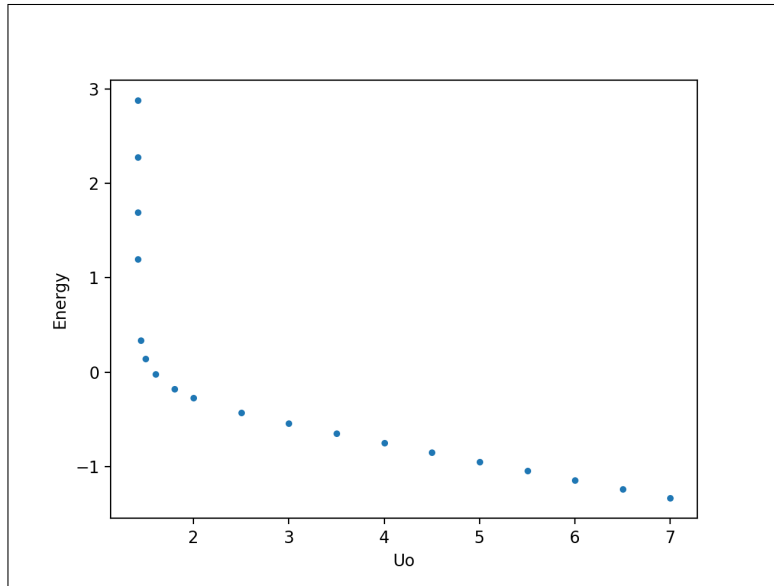


Figure 14: $E(U_0, \Sigma = 2)$

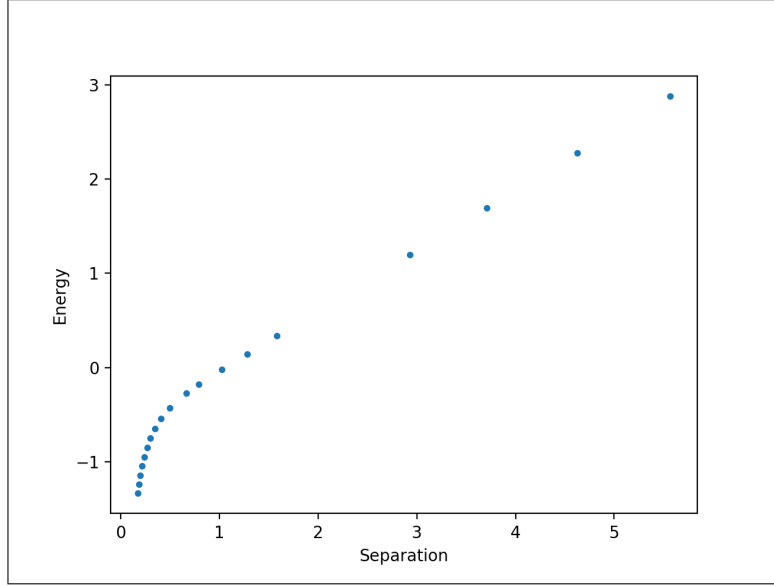


Figure 15: $E(L, \Sigma = 2)$

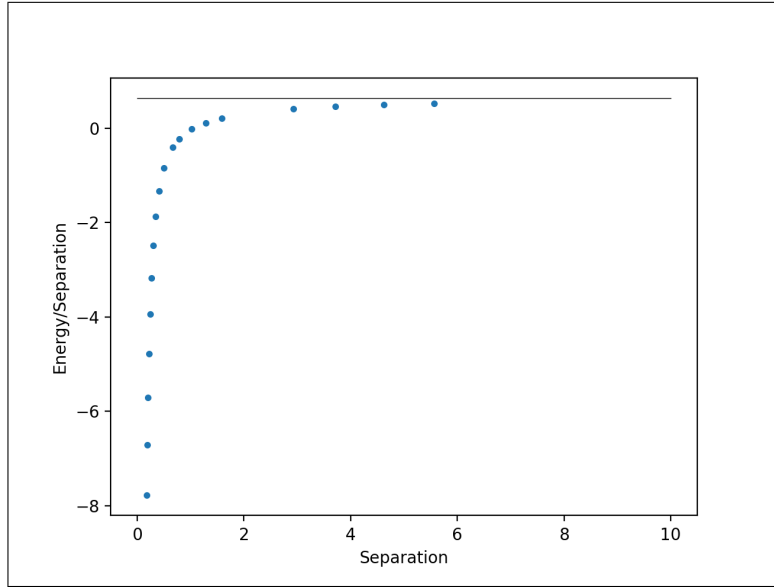


Figure 16: $E(U_0, \Sigma = 2)/L(U_0, \Sigma = 2)$, *BlackLine* = $2/\pi$

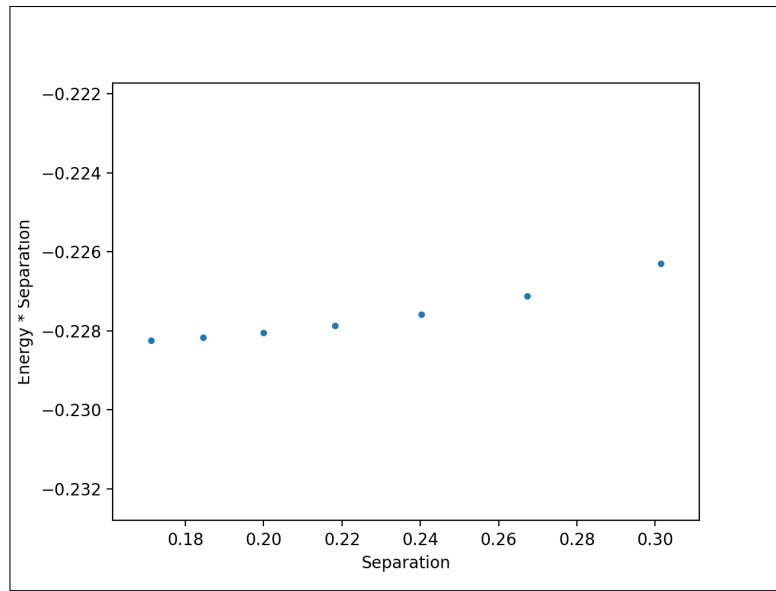


Figure 17: $E(U_0, \Sigma = 2) \cdot L(U_0, \Sigma = 2)$

$$\underline{\Sigma = 3}$$

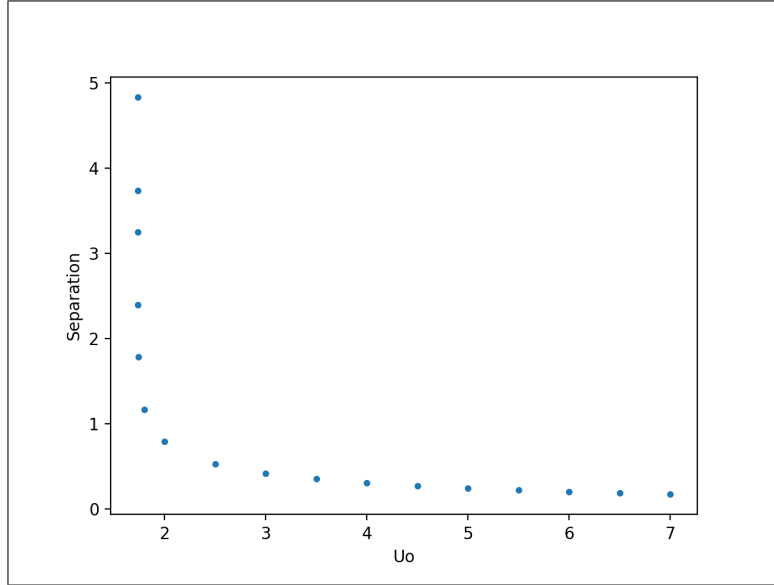


Figure 18: $L(U_0, \Sigma = 3)$

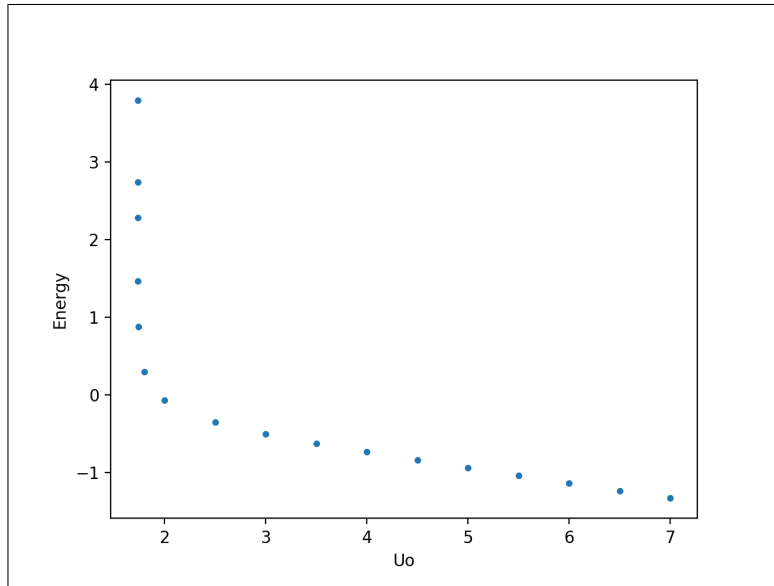


Figure 19: $E(U_0, \Sigma = 3)$

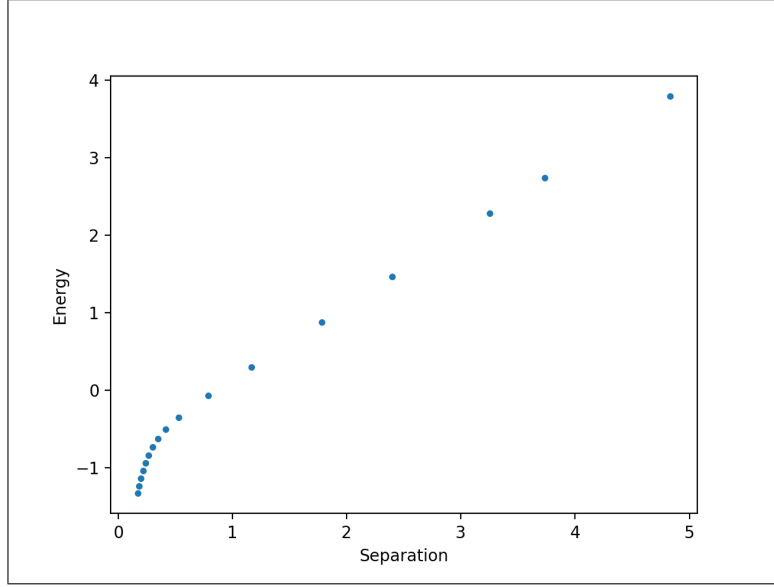


Figure 20: $E(L, \Sigma = 3)$

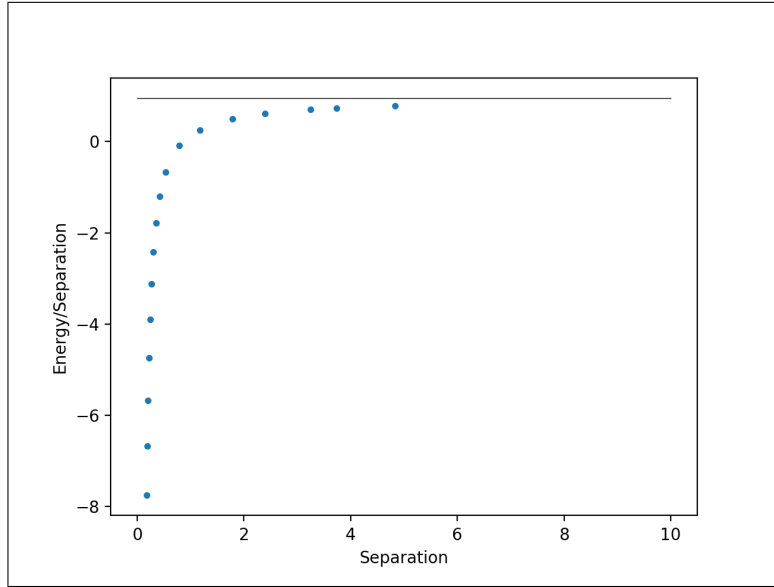


Figure 21: $E(U_0, \Sigma = 3)/L(U_0, \Sigma = 3)$, *BlackLine* = $3/\pi$

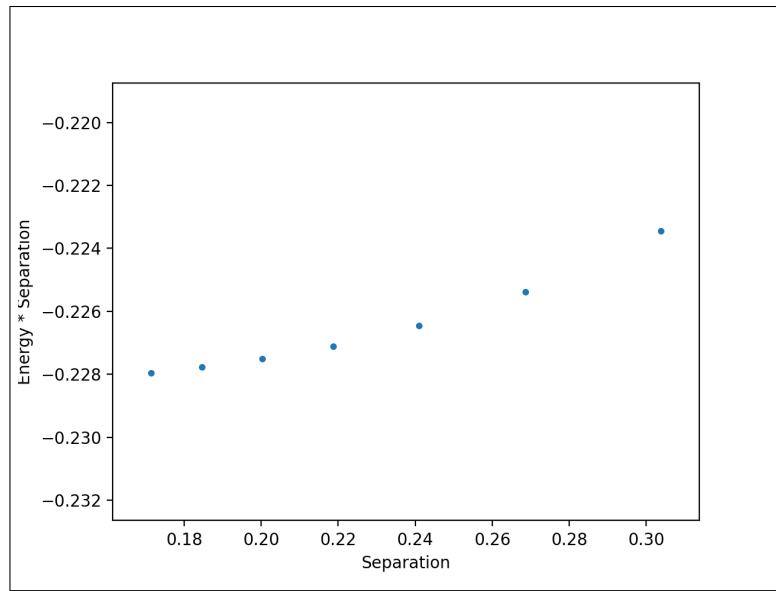


Figure 22: $E(U_0, \Sigma = 3) \cdot L(U_0, \Sigma = 3)$

$$\underline{\Sigma = 4}$$

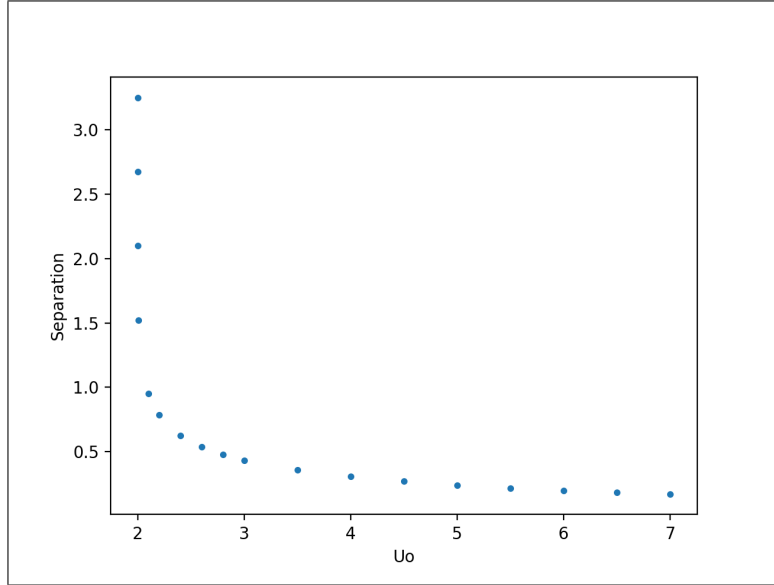


Figure 23: $L(U_0, \Sigma = 4)$

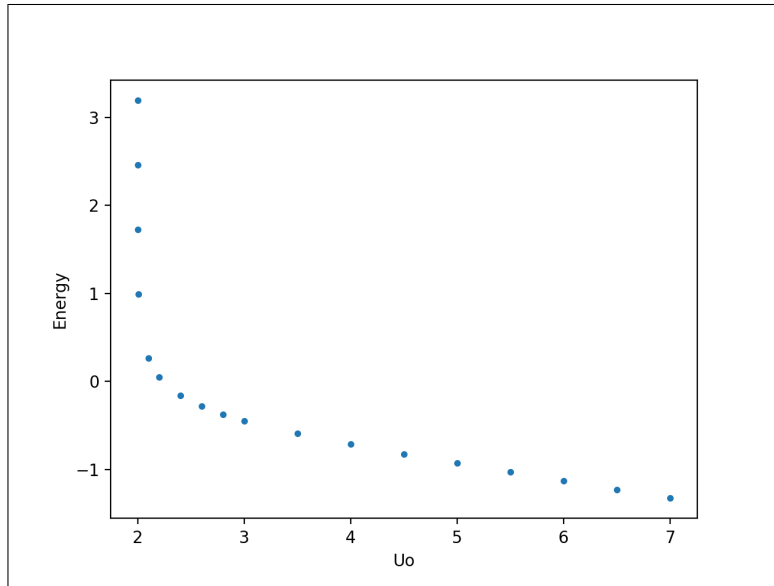


Figure 24: $E(U_0, \Sigma = 4)$

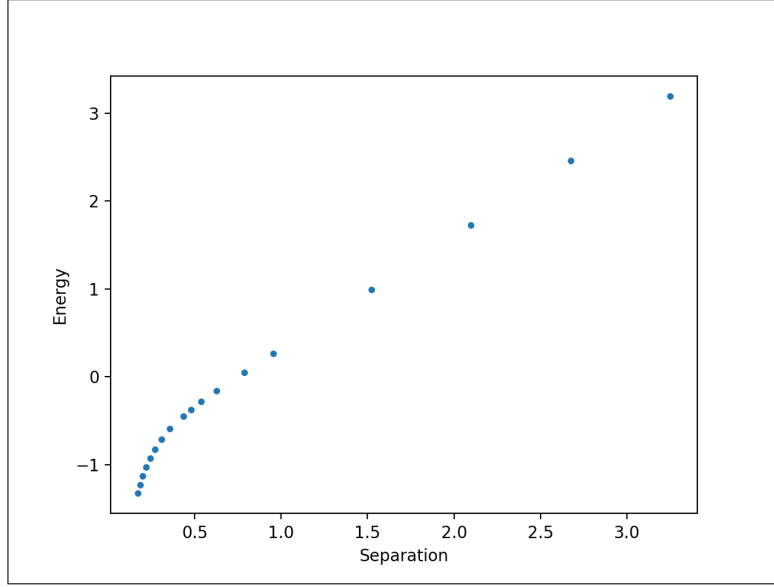


Figure 25: $E(L, \Sigma = 4)$

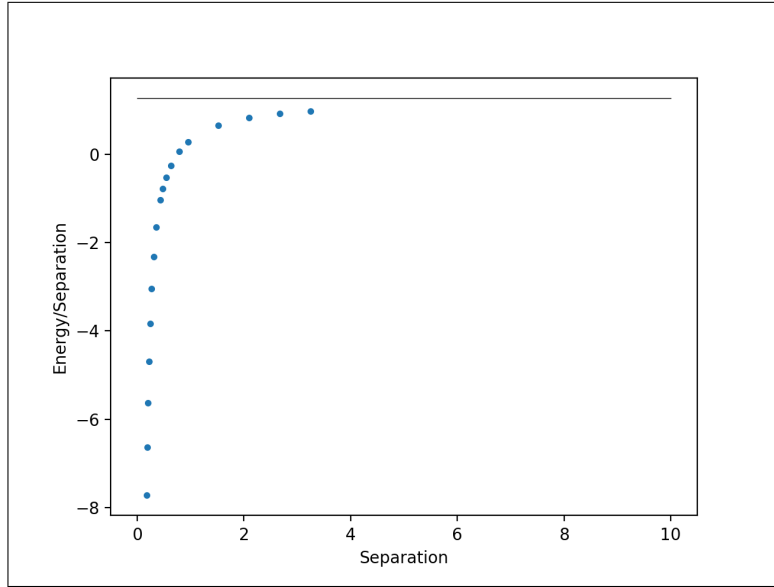


Figure 26: $E(U_0, \Sigma = 4)/L(U_0, \Sigma = 4)$, *BlackLine* = $4/\pi$

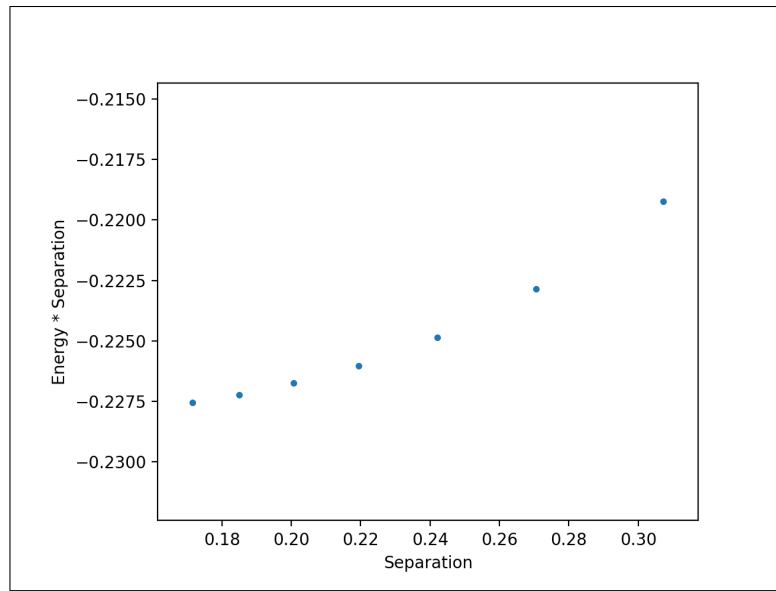


Figure 27: $E(U_0, \Sigma = 4) \cdot L(U_0, \Sigma = 4)$

$$\underline{\Sigma = 0}$$

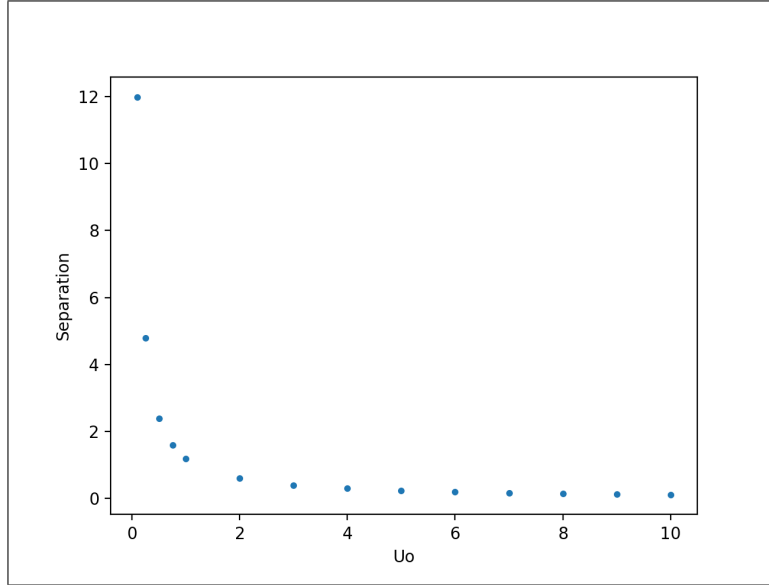


Figure 28: $L(U_0, \Sigma = 0)$

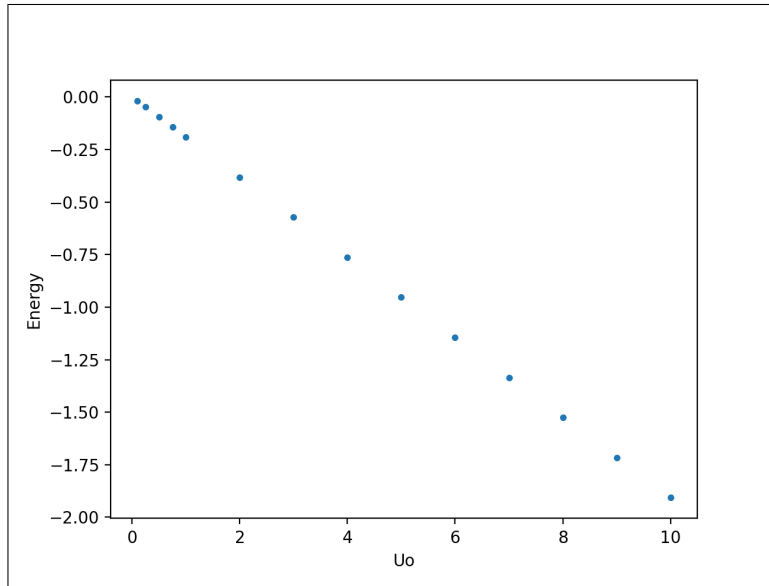


Figure 29: $E(U_0, \Sigma = 0)$

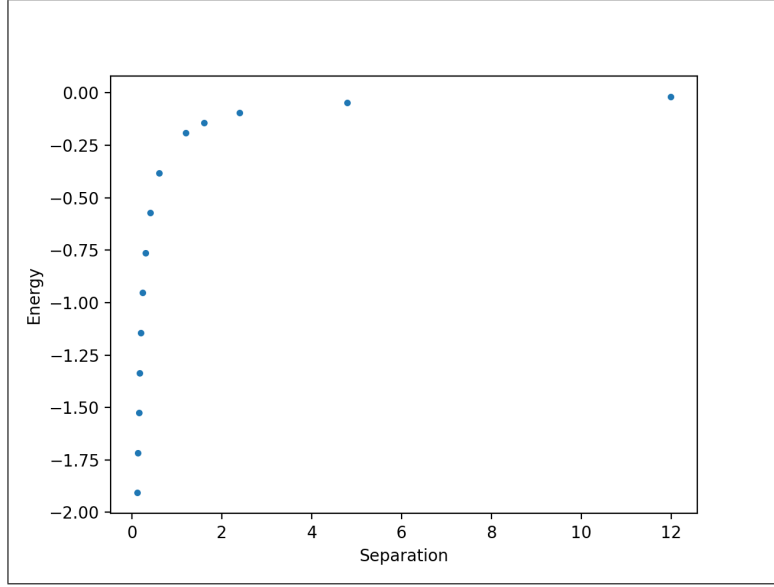


Figure 30: $E(L, \Sigma = 0)$

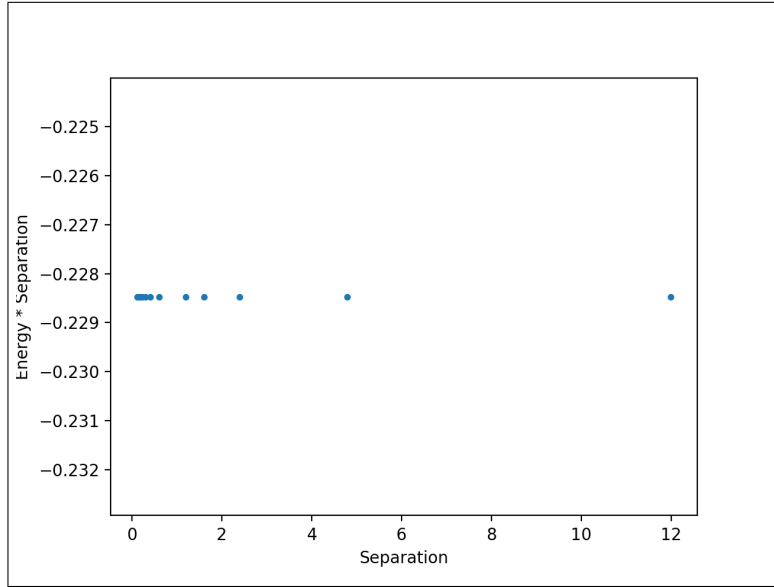


Figure 31: $E(U_0, \Sigma = 0) \cdot L(U_0, \Sigma = 0)$

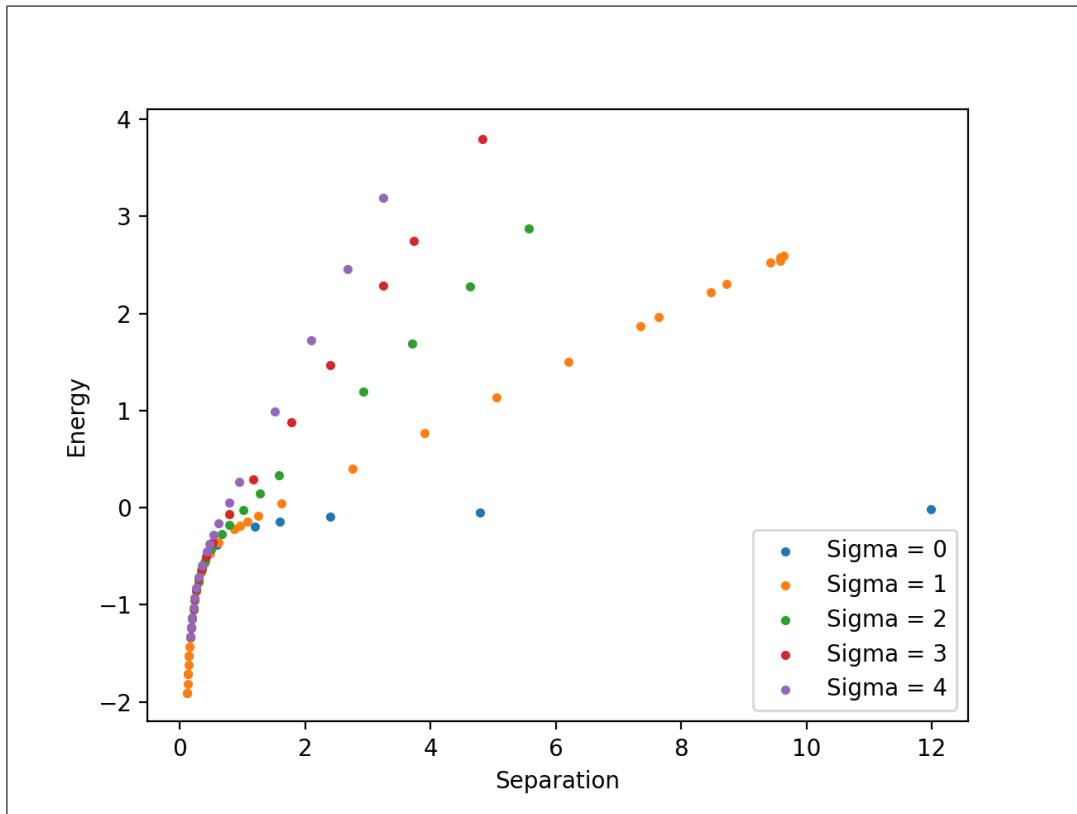


Figure 32: $E(L, \Sigma = 0, 1, 2, 3, 4)$